The Plant Journal (2004), **39**, 655–667 doi: 10.1111/j.1365-313X.2004.02164.x

Stromule formation is dependent upon plastid size, plastid differentiation status and the density of plastids within the cell

Mark T. Waters, Rupert G. Fray and Kevin A. Pyke*
Plant Sciences Division, University of Nottingham, Sutton Bonington Campus, Loughborough, LE12 5RD, UK

Received 26 April 2004; revised 4 June 2004; accepted 8 June 2004.
*For correspondence (fax 0115 95 16334; e-mail kevin.pyke@nottingham.ac.uk).

Summary

Stromules are motile extensions of the plastid envelope membrane, whose roles are not fully understood. They are present on all plastid types but are more common and extensive on non-green plastids that are sparsely distributed within the cell. During tomato fruit ripening, chloroplasts in the mesocarp tissue differentiate into chromoplasts and undergo major shifts in morphology. In order to understand what factors regulate stromule formation, we analysed stromule biogenesis in tobacco hypocotyls and in two distinct plastid populations in tomato mesocarp. We show that increases in stromule length and frequency are correlated with chromoplast differentiation, but only in one plastid population where the plastids are larger and less numerous. We used tobacco hypocotyls to confirm that stromule length increases as plastids become further apart, suggesting that stromules optimize the plastid–cytoplasm contact area. Furthermore, we demonstrate that ectopic chloroplast components decrease stromule formation on tomato fruit chromoplasts, whereas preventing chloroplast development leads to increased numbers of stromules. Inhibition of fruit ripening has a dramatic impact on plastid and stromule morphology, underlining that plastid differentiation status, and not cell type, is a significant factor in determining the extent of plastid stromules. By modifying the plastid surface area, we propose that stromules enhance the specific metabolic activities of plastids.

Keywords: stromule, plastid, tomato, plastid differentiation, *green flesh*, *ripening inhibitor*.

Introduction

Plastids are a family of interrelated organelles that assume various forms, such as chloroplasts, chromoplasts and amyloplasts, each with specialized roles and appearances which have formed the basis for their traditional classification (Waters and Pyke, 2004). In addition to photosynthesis, plastids are involved in numerous metabolic pathways including nitrate assimilation, starch metabolism and fatty acid biosynthesis (Neuhaus and Emes, 2000) and thus are integral to plant cell functionality. Recently, green fluorescent protein (GFP) and confocal microscopy has allowed the *in vivo* dynamics of subcellular organelles to be followed, providing a new approach to elucidate the complexities of plant cells (Hanson and Köhler, 2001; Hawes *et al.*, 2001; Köhler, 1998). The general view that plastids are separate, distinct cytoplasmic organelles was challenged following the expression of GFP targeted to the plastid stroma in tobacco and petunia plants. This revealed the presence of motile, thin protrusions, emanating from the plastid surface into the surrounding cytoplasm (Köhler *et al.*, 1997). These protrusions, now known as *stromules* (stroma-filled tubules), sometimes link individual plastids and allow them to exchange macromolecules (Kwok and Hanson, 2004a). Although evidence of such plastid shape dynamics has been reported sporadically in the past (Gray *et al.*, 2001), modern microscopy techniques coupled with GFP have allowed the reliable study of the motile nature of both pigmented and non-pigmented plastids in a wide variety of plant species. Since their initial re-discovery (Köhler *et al.*, 1997), stromules have been reported in several angiosperm species including *Arabidopsis* (Hibberd *et al.*, 1998; Tirlapur *et al.*, 1998), wheat (Langeveld *et al.*, 2000), rice (Bourett *et al.*, 1999) and tomato (Pyke and Howells, 2002). An overview of plastid morphology in various tobacco cell types revealed that stromules are distributed in a tissue-specific manner,

with an emergent trend that stromules are most abundant on non-green plastids such as those found in roots and cultured suspension cells (Köhler and Hanson, 2000). Conversely, chloroplasts such as those in leaf mesophyll cells exhibit few stromules, and these tend to be short and ephemeral in nature. However, such observations suffer from the problem of confounding factors, as non-green plastids are often present at lower numbers within the cell and are frequently smaller; in these cells stromules might help increase the surface area for plastid–cytoplasm contact. Furthermore, cellular differentiation, in conjunction with plastid differentiation, may also influence stromule biogenesis.

Chromoplasts are a class of plastids specialized in the synthesis and accumulation of coloured carotenoids (Camara *et al.*, 1995). In tomato fruit, chloroplasts differentiate into chromoplasts upon the initiation of ripening, a process which occurs over about 7 days (Fraser *et al.*, 1994). Chlorophyll is degraded and carotenoids such as β-carotene and lycopene are deposited in membranous inclusions within the developing chromoplast (Cheung *et al.*, 1993; Harris and Spurr, 1969). While the biochemistry of chromoplasts has been studied extensively (Camara *et al.*, 1995), the cell biology and population dynamics of chromoplasts have received little attention. This is surprising, given the many attempts to improve the nutritional value of tomatoes by modifying their carotenoid content (Bramley, 1997; Römer *et al.*, 2000). Analysis of plastid division in tomato fruit revealed that the majority of plastid division occurs during the fruit enlargement stages when the plastids are present as chloroplasts, such that plastid number remains fairly constant once ripening commences (Cookson *et al.*, 2003). In terms of chromoplast morphology, we showed previously that although stromules are relatively rare on chloroplasts in green fruit, they frequently form highly complex structures that appear to interlink individual chromoplasts in ripe fruit (Pyke and Howells, 2002).

To understand the functions of stromules and the reasons underpinning their variability, it is necessary to document the changes in stromule morphology that occur during the process of plastid differentiation both within and between different cell types, as both plastid type and cell type might influence stromule biogenesis. The tomato fruit represents a good system for studying stromules because (i) there is a well-defined plastid transition from the chloroplast to chromoplast; (ii) tomato fruit is composed of several different cell types that undergo the same plastid differentiation process; and (iii) there exist several mutants of tomato that alter various aspects of the fruit ripening process and the plastid differentiation pathway. In this study we show that stromule abundance increases following the chloroplast to chromoplast transition but only in cells where plastids are large and further apart. This induction is prevented in a ripening-deficient mutant where plastid development is blocked. We investigate the influence of a chloroplast-like environment on stromule formation, and demonstrate that there is a negative correlation between the retention of chloroplast components and stromule abundance. Finally, we confirm using tobacco seedlings that stromule formation is dependent on the number of plastids per unit area of the cell. We propose that there are multiple, interacting factors which determine the frequency and extent of stromules in plant cells, and that the abundance of stromules in ripe tomato fruit may be a significant feature of chromoplast activities.

Results

Two distinct plastid populations exist in the mesocarp of tomato fruit

Developing tomato fruit can be classified according to size and colour. The four stages we consider here cover the transition from chloroplast to chromoplast in a mature (i.e. full-sized) fruit. At mature green (MG), fruit enlargement has ceased. Breaker (B) marks the initiation of ripening when the first colour change becomes apparent; all subsequent stages are defined as days post-breaker (i.e. B + 1, B + 3, B + 7; Figure 1a). By B + 7 an 'Ailsa Craig' tomato fruit is ripe, with almost maximal levels of carotenoids and little or no remnant chlorophyll (Fraser *et al.*, 1994). The pericarp of tomato fruit consists of a thick layer of large, vacuolated cells immediately beneath the epidermis, and has three distinct sub-regions: the exocarp, the mesocarp and the endocarp (Gillaspy *et al.*, 1993; Figure 1b). The exocarp is composed of two to three layers of parenchymatous cells. Internal to this are several layers of large mesocarp cells that make up the majority of the pericarp, within which is found an apical-basal vascular system, distributed throughout the fruit in a regular manner rather like the lines of longitude on a globe. The innermost region, the endocarp, is a single layer of cells that lines the locules where the seeds develop. Inspection of whole pericarp sections from MG fruit expressing the stroma-targeted GFP construct reveals that the vasculature appears to delineate two distinct cell types within the mesocarp itself (Figure 1b).

In MG fruit, the mesocarp cells outermost to the vasculature (outer mesocarp or OM cells) possess small, numerous chloroplasts, whereas those towards the interior of the fruit (inner mesocarp or IM cells) contain large, starch-filled plastids that are fewer in number (as indicated by staining with potassium iodide/iodine solution; data not shown and Figure 2). This plastid dimorphism is maintained throughout the fruit ripening process with major differences in plastid size, morphology and number per unit area (Figure 2; Table 1). In ripe fruit (B + 7), the chromoplasts in OM and IM cells are highly distinct. In OM cells, chromoplasts often take on an oblong, needle-like appearance (Figure 2g), whereas IM-cell chromoplasts are much larger and ovoid in shape (Figure 2h). The different cell populations and

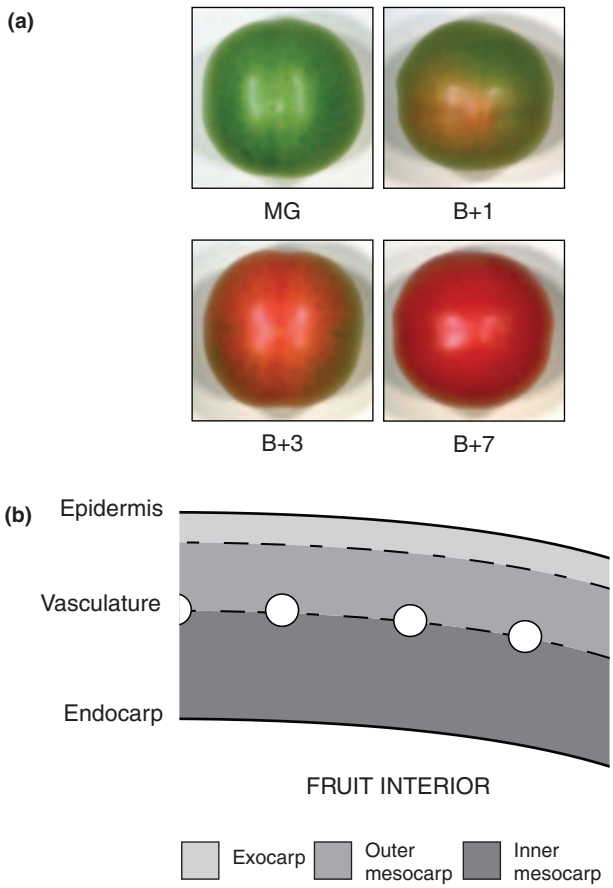

Figure 1. Tomato fruit development and pericarp structure.
(a) Representative fruit from each of the four stages of ripening considered. Note the slight colour change that is visible in B + 1, indicating the start of chromoplast differentiation.
(b) Part of a longitudinal section through a full-sized tomato fruit pericarp. The pericarp is the fleshy wall of the fruit. The epidermis and endocarp are both single cell layers, and are depicted by solid lines. Dashed lines indicate approximate boundaries between the different layers; the mesocarp is divided into two sub-regions based on plastid morphology and cell size (here termed outer and inner mesocarp). The two sub-regions are approximately delineated at the level where the vasculature pervades the mesocarp.

stages of fruit ripening are also associated with dramatic shifts in stromule morphology. In MG fruit, stromules in IM cells tend to be much longer and conspicuous than those in OM cells (Figure 2, insets). Stromules in MG OM cells are often stubby and do not protrude far into the cytoplasm, with a mean length of 5.6 μm (Table 1). These are reminiscent of stromules found on chloroplasts in tissues such as mesophyll cells and trichomes (data not shown). However, stromules in IM cells of MG fruit can be extremely long, with a mean length of 13.5 μm (Table 1). These OM–IM cell differences are maintained at all stages, but the distinction is most pronounced once ripening commences (Figure 2, insets). Stromules are longest in IM cells from B + 7 fruit, and there is often more than one stromule per chromoplast in this cell type (Figure 2h). In addition, IM cells frequently show variably sized vesicles that are not directly associated with plastids or stromules, and which contain GFP but not chlorophyll (Figure 2). We suspect that these vesicles may be formed following the collapse of long stromules, as OM cells (with short stromules) do not possess them. It should also be noted that IM cell plastids from MG, B + 1 and B + 3 fruit show considerable intracellular variability in size (Table 1; Figure 2). This may be caused by rapid mobilization of starch reserves that commences just prior to breaker and proceeds through ripening (Büker *et al.*, 1998). Furthermore, the changes in plastid morphology may be compounded by incomplete thylakoid degradation and varying degrees of plastid differentiation. Such metabolic and developmental events are presumably not simultaneous throughout the fruit or even within a cell, leaving a heterogeneous population of plastids of different sizes and differentiation status.

Stromule frequency and length varies with plastid size and type

To investigate further how stromule abundance changes during ripening, we measured the stromule frequency (i.e. the proportion of plastids with stromules) and stromule length in both OM and IM cells at each of the four stages of wild type fruit development. Stromule frequency is expressed as 'stromule index' for quantification (see Experimental procedures). In addition, other parameters such as plastid size and plastids per unit area (a measure of plastid density within the cell; hereafter termed 'plastid index') were determined (Table 1).

The stromule index is significantly lower in OM cells than in IM cells at all stages post-breaker (Mann–Whitney rank sum test, $P > 0.05$; Figure 3a), except in the case of MG fruit where there is no significant difference. The pattern of stromule index as ripening progresses differs between each of the two cell types. In OM cells, stromule index remains approximately constant throughout fruit development with only small changes. However, in IM cells there is a large and significant increase in stromule frequency upon the initiation of ripening, that is between MG and B + 1, where the proportion of plastids with stromules rises from 7 to 32%, respectively (Mann–Whitney, $P < 0.001$; Figure 3a and Table 1). After the B + 1 stage, stromule frequency in IM cells remains high and approximately constant with no significant change. From these data we infer that there is a dramatic increase in stromule frequency during the differentiation of chloroplasts to chromoplasts, but that this change is IM cell-specific.

Stromule length also varies between both cell types during fruit development. In OM cells, stromule length remains constant across all fruit stages, although there appears to be a transitory and significant increase at B + 3 (Mann–Whitney, $P < 0.001$; Figure 3b). This may be caused

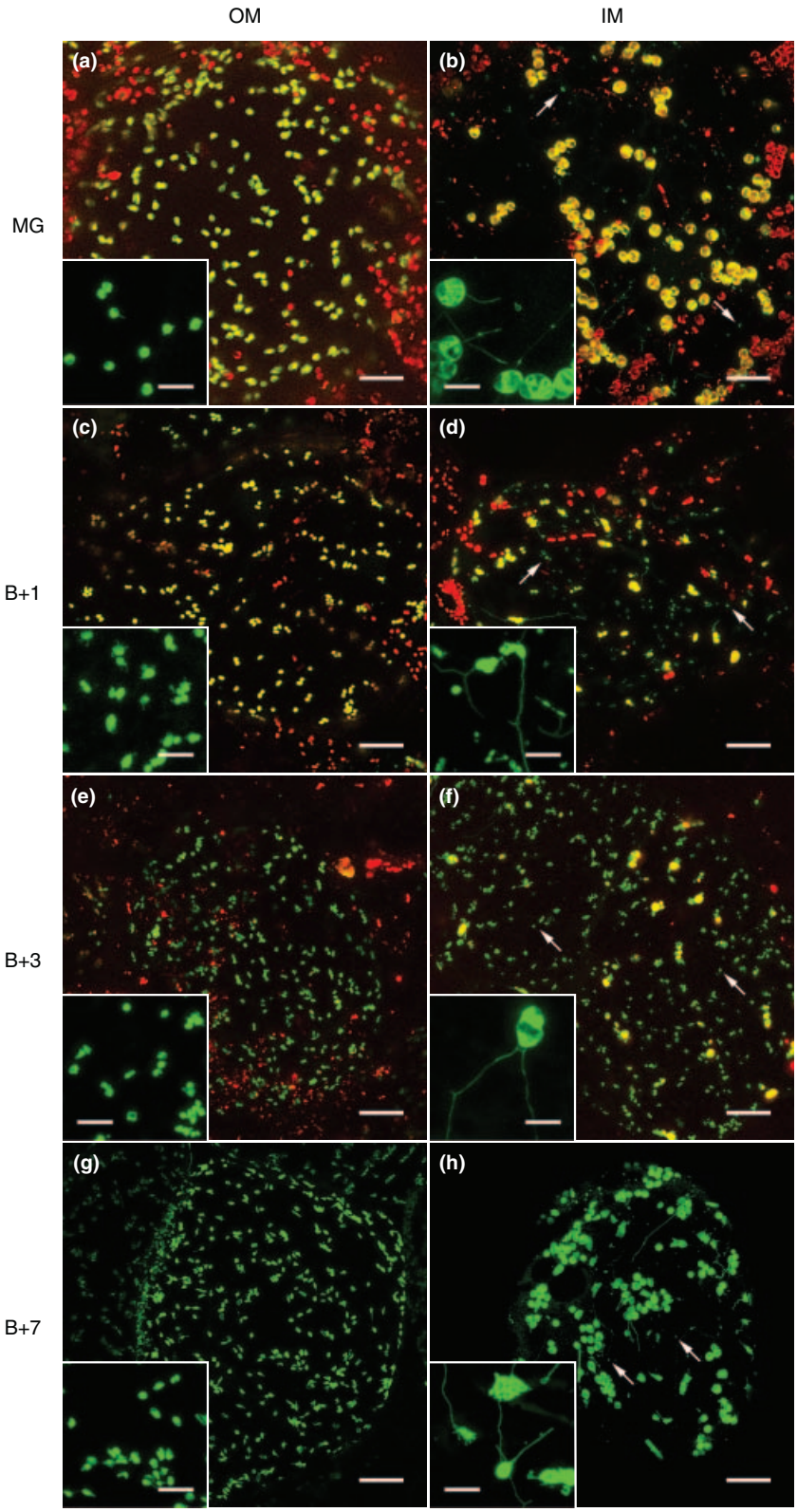

Figure 2. Changes in plastid and stromule morphology during ripening.
Confocal maximum projections of individual cells from the outer mesocarp (OM) and inner mesocarp (IM) at various stages of ripening [MG, mature green; B + 1, B + 3, B + 7, 1, 3 and 7 day(s) post-breaker, respectively]. Insets show higher magnifications of representative cells. With the exception of (g), (h) and the insets, all images show a combination of green fluorescent protein (GFP) and chlorophyll autofluorescence signals false-coloured green and red, respectively, with yellow representing overlap. Note the consistent difference in plastid size between OM and IM cells at each stage, and the IM-cell-specific plastid-derived vesicles which show GFP signal only (b, d, f, h, arrows). Scale bars: main images, 40 μm; insets, 10 μm.

Table 1 Stromule abundance, plastid size and plastid index in tomato fruit mesocarp cells

Genotype	Stage	Cell type	n[a]	Mean stromule frequency (%)[b]	Mean stromule length (μm)[c]	Max stromule length (μm)[d]	Mean plastid plan area (μm^2)[e]	Plastid index (plastids per 10 000 μm^2)[f]
WT	MG	OM	23	12	5.6 ± 0.3	28	24.0 ± 1.2	27.2 ± 2.6
		IM	24	7	13.5 ± 1.2	70	49.0 ± 3.2	17.2 ± 1.3
	B + 1	OM	12	8	4.8 ± 0.5	22	20.2 ± 1.3	29.8 ± 2.4
		IM	15	32	31.7 ± 3.2	180	38.1 ± 2.6	11.6 ± 1.5
	B + 3	OM	15	12	11.1 ± 1.2	52	22.8 ± 1.3	20.7 ± 2.6
		IM	15	32	37.6 ± 3.8	220	42.9 ± 2.8	10.7 ± 1.6
	B + 7	OM	18	5	5.8 ± 0.6	36	19.6 ± 1.1	32.9 ± 2.9
		IM	21	39	32.6 ± 1.9	180	40.7 ± 1.8	12.7 ± 1.4
WT [dark grown]	MG	OM	10	25	4.7 ± 0.5	20	17.4 ± 0.9	18.6 ± 1.1
		IM	10	12	11.3 ± 1.8	50	52.0 ± 4.3	11.7 ± 1.3
gf	B + 7	OM	17	8	6.2 ± 0.8	59	21.0 ± 1.1	30.6 ± 2.6
		IM	22	27	39.2 ± 2.9	200	54.9 ± 3.6	7.0 ± 2.8
rin	~B + 40	OM	11	15	2.4 ± 0.1	5.1	10.4 ± 0.2	45.4 ± 7.1
		IM	10	19	2.7 ± 0.1	4.9	12.9 ± 0.3	41.1 ± 7.2

[a]Number of cells used to calculate stromule index.
[b]Mean proportion of plastids with stromules from *n* cells.
[c]Mean ± 1 SE of measurements from at least five stromules from each of the *n* cells.
[d]Maximum stromule length across all *n* cells.
[e]Mean ± 1 SE of measurements from five plastids from each of the *n* cells.
[f]Mean ± 1 SE of measurements from *n* cells.

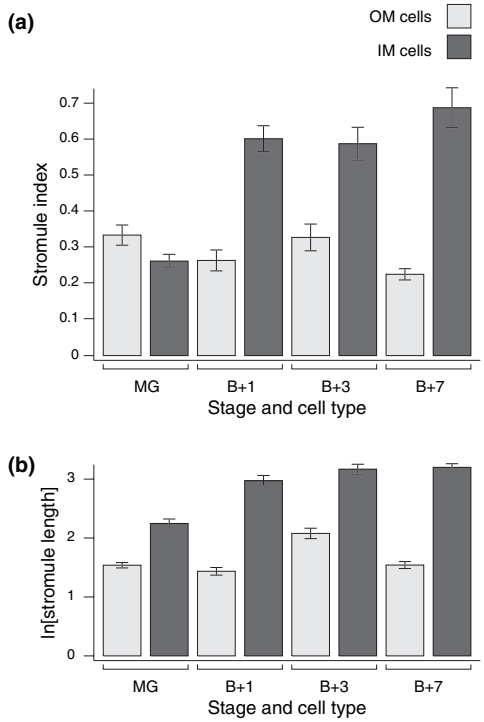

Figure 3. Changes in stromule frequency and length in wild type tomato fruit during ripening.
(a) Stromule index (a measure of stromule frequency; see Experimental procedures).
(b) Stromule length plotted on a logarithmic scale. Bar heights show mean and error bars signify ±1 SE.

by plastids in fruit of this stage being intermediate between chloroplast and chromoplast, leading to discrepancies in plastid morphology that are typical of neither the mature chloroplast nor chromoplast. However, in IM cells stromule length is consistently and significantly higher than in the corresponding OM cells at all stages of fruit development considered (Figure 3b). Furthermore, there is an increase in stromule length upon the transition from MG to B + 1, and still a further increase between B + 1 and B + 7 (Mann–Whitney, $P < 0.001$ and $P = 0.02$, respectively; Figure 3b). This suggests that the transition from chloroplast to chromoplast correlates with increased stromule length but only in IM cells.

The green flesh mutation reduces stromule frequency in IM cells of ripe fruit

As chloroplasts generally produce fewer and shorter stromules than non-green plastid types (Gray *et al.*, 2001; Köhler and Hanson, 2000), we hypothesized that experimentally maintaining a chloroplast-like plastid status might inhibit stromule formation in ripe fruit mesocarp cells. To test this, we introduced the plastid-targeted GFP construct into the *green flesh* (*gf*) mutant background. This mutant is deficient in the removal of chlorophyll and thylakoid complexes from the developing chromoplast (Cheung *et al.*, 1993) as well as from chloroplasts in senescing leaves (Akhtar *et al.*, 1999). In wild type fruit, the photosynthetic apparatus is removed from the chloroplast upon ripening. In *gf* this process takes

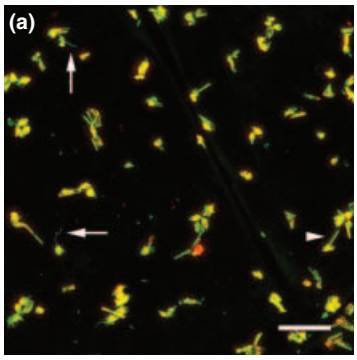

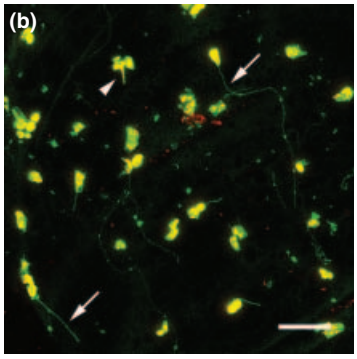

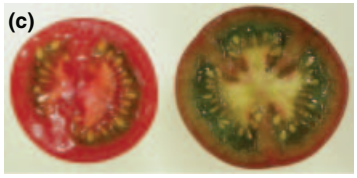

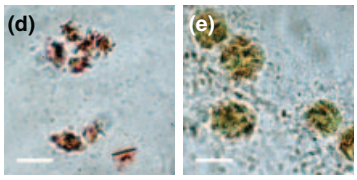

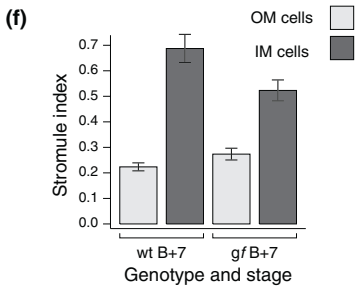

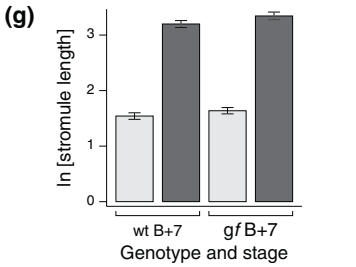

very much longer: by B + 7 both carotenoids and chlorophyll are present in the pericarp plastids, resulting in a dirty-red fruit colour (Figure 4c, e). Plastids in such fruit thus possess properties of both chloroplasts and chromoplasts (Cheung *et al.*, 1993).

At B + 7, stromules in *gf* fruit appear similar to wild type, being rare in OM cells but relatively common and extensive in IM cells (Figure 4a, b). However, quantitative measurements revealed that the mutation has mixed effects on both stromule index and length. Stromules are more rare in IM cells of *gf* B + 7 fruit than in wild type (27% versus 39% of plastids possess stromules, respectively; Table 1 and Figure 4f), and this difference, although small, is significant (Mann–Whitney, $P = 0.02$). The effect on stromule index in OM cells is apparently the opposite (Figure 4f), but this difference is not significant ($P = 0.15$). In terms of stromule length, there are no significant differences between *gf* and wild type in either OM or IM cells (Figure 4g). Furthermore, parameters such as mean and maximum stromule length remain much the same in *gf* as in wild type (Table 1). It is notable that both the physical appearance of plastids and stromules, as well as the frequencies and lengths of stromules from *gf* fruit, are comparable with those obtained from ripening wild type fruit (compare, for example, Figure 2d with Figure 4b): in both of these situations plastid differentiation is incomplete, with morphologies intermediate between chloroplast and chromoplast. Collectively, these findings suggest that maintaining the chloroplast state reduces the tendency for stromule formation.

Inhibiting chloroplast development increases stromule frequency in a cell type-specific manner

To address further the effects of the chloroplast state on stromule formation, we inhibited chloroplast differentiation by preventing light from reaching the post-fertilization flower. This blocks chloroplast differentiation, resulting in a white fruit that is morphologically normal when compared with light-grown fruit at the equivalent MG stage (Figure 5c). Fruit grown in this way will develop as normal and ripen fully, suggesting that the light signal is not required for chromoplast differentiation (data not shown). A large induction in stromule frequency relative to light-grown fruit

Figure 4. Plastid and stromule morphology in *gf* B + 7 fruit.
Confocal images of representative (a) outer mesocarp (OM) cells and (b) inner mesocarp (IM) cells from B + 7 *gf* fruit. Green fluorescent protein (GFP) and chlorophyll autofluorescence signals are false-coloured green and red, respectively, with yellow representing overlap. Note that stromules (arrows) and lycopene crystal deformations (arrowheads) are different in width and regularity in shape. (c) Wild type (left) and *gf* B + 7 fruit sections. Note the brown-red colour of the *gf* pericarp. Brightfield images of (d) wild type and (e) *gf* plastids show the differences in pigmentation responsible for the fruit colour. Note the presence of both lycopene crystals and chlorophyll in *gf* plastids. (f) Stromule index and (g) stromule length in wild type (wt) and *gf* B + 7 fruit. Bar heights represent the mean ± 1 SE. Scale bars: (a), (b): 40 μm; (d), (e): 10 μm.

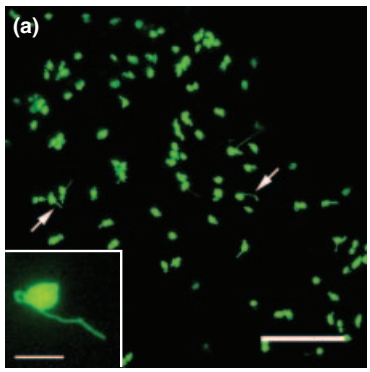

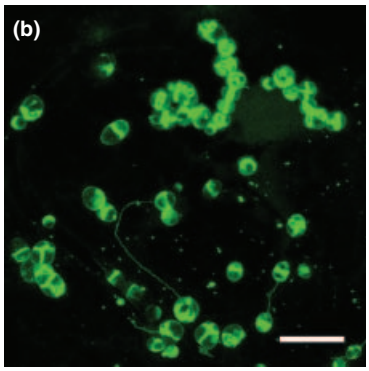

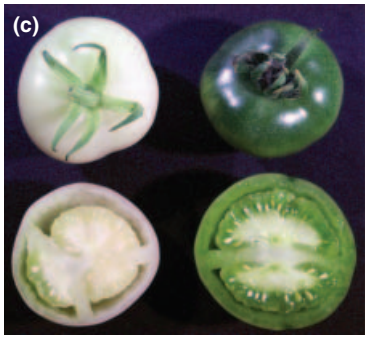

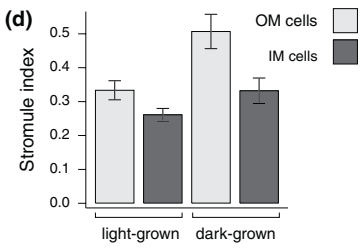

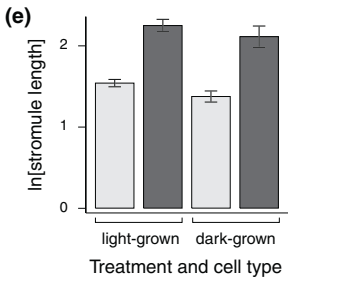

was observed in OM cells of dark-grown fruit (Figure 5a), but this difference was not so apparent in IM cells in which the plastids retained their large, starchy appearance with few, relatively long stromules (Figure 5b). Image analysis confirmed this observation: within OM cells, stromule index was significantly higher in dark-grown than light-grown fruit (Mann–Whitney, $P = 0.007$), but not different in IM cells ($P = 0.07$; Figure 5d). Stromule length in IM cells did not vary significantly between the two treatments ($P = 0.39$) and, surprisingly, there was no significant difference in stromule lengths in OM cells between dark and light-grown fruit ($P = 0.22$; Figure 5e). From these data we conclude that preventing chloroplast differentiation leads to more stromules, but that this can be modulated by other factors, as IM cell plastids in MG fruit retain their morphological characteristics whether or not they are chloroplastic.

The rin mutation dramatically decreases stromule abundance in tomato fruit

Whereas the *gf* mutation affects only a specific aspect of fruit ripening, the *ripening inhibitor* (*rin*) mutation disrupts ripening in a more global fashion. *rin* fruit develop normally until breaker whereupon they gradually lose chlorophyll and turn yellow, but do not accumulate lycopene, having reduced carotenoid levels in general (Tigchelaar *et al.*, 1978). Furthermore, *rin* fruit do not undergo the respiratory climacteric, and remain firm at all stages of development. *RIN* encodes a MADS-box transcription factor which is predicted to operate upstream of the ethylene signalling cascade which triggers the ripening response (Vrebalov *et al.*, 2002). Given this fundamental arrest of fruit development, we used the *rin* mutant to investigate the effects of blocking ripening on plastid and stromule morphology.

We introduced the *gfp* transgene into the *rin* mutant background by crossing. Plastid morphology is indistinguishable from that of wild type during the green stages of fruit development before breaker is reached, with the mesocarp plastid dimorphism readily apparent in MG fruit (data not shown). By 40 days post-breaker, *rin* fruit are hard and yellow (Figure 6c), and the plastids lose their chlorophyll (Figure 6d). Much of the plastid dimorphism is lost by

Figure 5. Plastid and stromule morphology in dark- and light-grown mature green fruit.
(a) Confocal maximum projection of an outer mesocarp (OM) cell from dark-grown fruit; stromules are arrowed. Inset: epifluorescence micrograph of a representative plastid from this tissue, showing a lack of chlorophyll autofluorescence.
(b) Confocal maximum projection of an inner mesocarp (IM) cell from dark-grown fruit. Note the prominent starch grains causing patchiness of green fluorescent protein (GFP) fluorescence.
(c) Representative image of dark-grown and light-grown fruit at approximately similar (MG) stages of development.
(d) Stromule index and
(e) Stromule length in dark- and light-grown fruit. Bar heights represent the mean ± 1 SE. Scale bars: A: 40 μm (inset 5 μm); B: 40 μm.

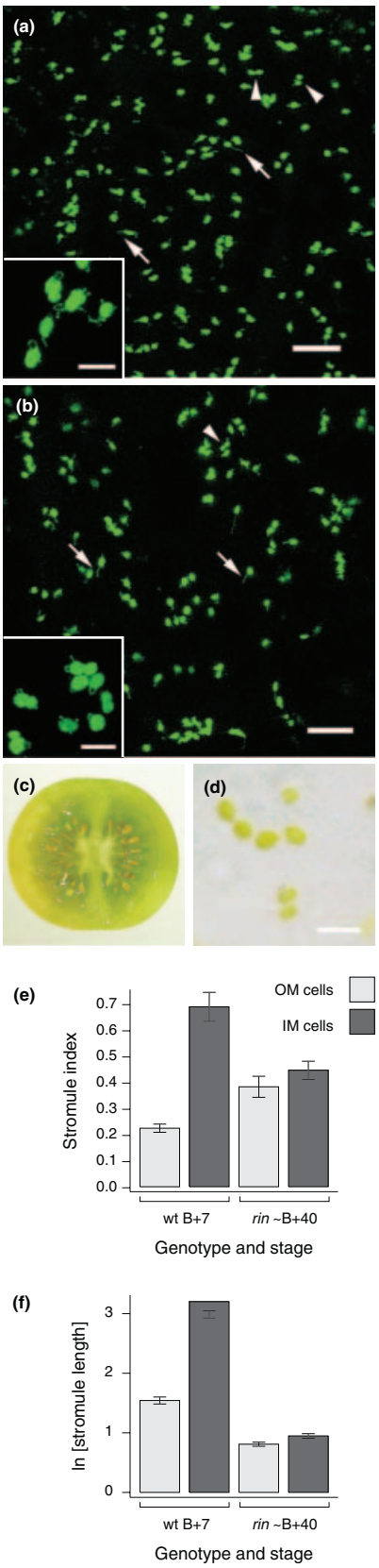

this stage: in both IM and OM cells, plastid size and index are similar, but dramatically different from wild type when compared with either MG or B + 7 fruit (Table 1). The plastids in yellow *rin* fruit are small and numerous in comparison with wild type mesocarp cells, and are relatively regular in shape. Moreover, the plastids in yellow *rin* fruit often appear in a state of division (Figure 6a,b); this is supported by the greatly increased plastid index and reduced plastid size (Table 1).

The loss of plastid dimorphism across the mesocarp is reflected in the stromule architecture in *rin* fruit: long, extensive stromules are entirely absent and are replaced by limited protrusions that often form loops (Figure 6a,b). When analysed quantitatively, the OM–IM differences in stromule index largely disappear, with no significant difference between these two cell types in B + 40 *rin* fruit (Mann–Whitney, $P = 0.22$). Furthermore, relative to wild type B + 7 fruit, stromules are less common in IM cells but more so in OM cells of *rin* fruit (Figure 6e). Stromules are much shorter in *rin* B + 40 fruit than in wild type B + 7 fruit in both IM and OM cells, but there is still a small and significant difference in stromule length between OM and IM cells within the mutant fruit (Mann–Whitney, $P = 0.01$; Figure 6f and Table 1). This suggests that, although much reduced relative to wild type, there remains some aspect of plastid dimorphism even at this late stage of fruit development. From these data we conclude that the *rin* mutation has a major impact on stromule morphogenesis. As the stromules are frequently observed extending and retracting into the cytoplasm (data not shown), the basic machinery for stromule formation and movement are not compromised in this mutant. Therefore, we conclude that the dramatic effects on stromule formation are an indirect result of a block on plastid development.

Stromule length is negatively correlated with plastid density

The differences in stromule length and frequency between OM and IM cells suggest that plastid index may be a determining factor in stromule formation. In order to test the hypothesis that stromules become more abundant when plastids are further apart, we switched to another system based on tobacco hypocotyls. During skotomorphogenesis, the hypocotyl elongates and the epidermal cells expand but do not divide (Gendreau *et al.*, 1997). To produce a range of plastid index values, seeds were sown on nutrient agar media

Figure 6. Plastid and stromule morphology in *rin* fruit at B + 40.
Confocal maximum projections of (a) outer mesocarp (OM) and (b) inner mesocarp (IM) cells from full yellow B + 40 *rin* fruit. Note the conspicuously small plastids and short stromule protrusions (arrows). Some plastids appear to have divided recently (arrowheads). Insets show loops and short protrusions typical in this mutant. (c) Cross-section of a representative *rin* fruit and (d) brightfield image of typical plastids. (e) Stromule index and (f) stromule length in *rin* B + 40 fruit compared with wild type B + 7 fruit. Bar heights represent the mean ± 1 SE. Scale bars: (a), (b): 20 μm (insets 10 μm); (d): 10 μm.

and germinated in the dark for 5, 6, 7 or 9 days, and then transferred to light for a further day. The day of light treatment enhanced expression of the GFP transgene and inhibited further hypocotyl elongation. This resulted in seedlings with a wide range of hypocotyl lengths, which were then examined for stromule morphology in the epidermal cells (Figure 7a–e). Stromules were abundant in all treatments and usually protruded in the direction of cell elongation, that is in parallel with the lateral cell walls (Figure 7a–d).

We observed a significant trend in plastid morphology as hypocotyl length increased. At 6 days post-germination (dpg; this comprises 5 days dark and 1 day light), the hypocotyl exhibited slight elongation and the epidermal plastids frequently produced stromules with a mean length of 6 μm (Figure 7a,f). Longer dark periods led to greater hypocotyl elongation and more dispersed epidermal plastids, and stromules were significantly longer on average (Mann–Whitney, $P < 0.05$). However, at 8 and 10 dpg there

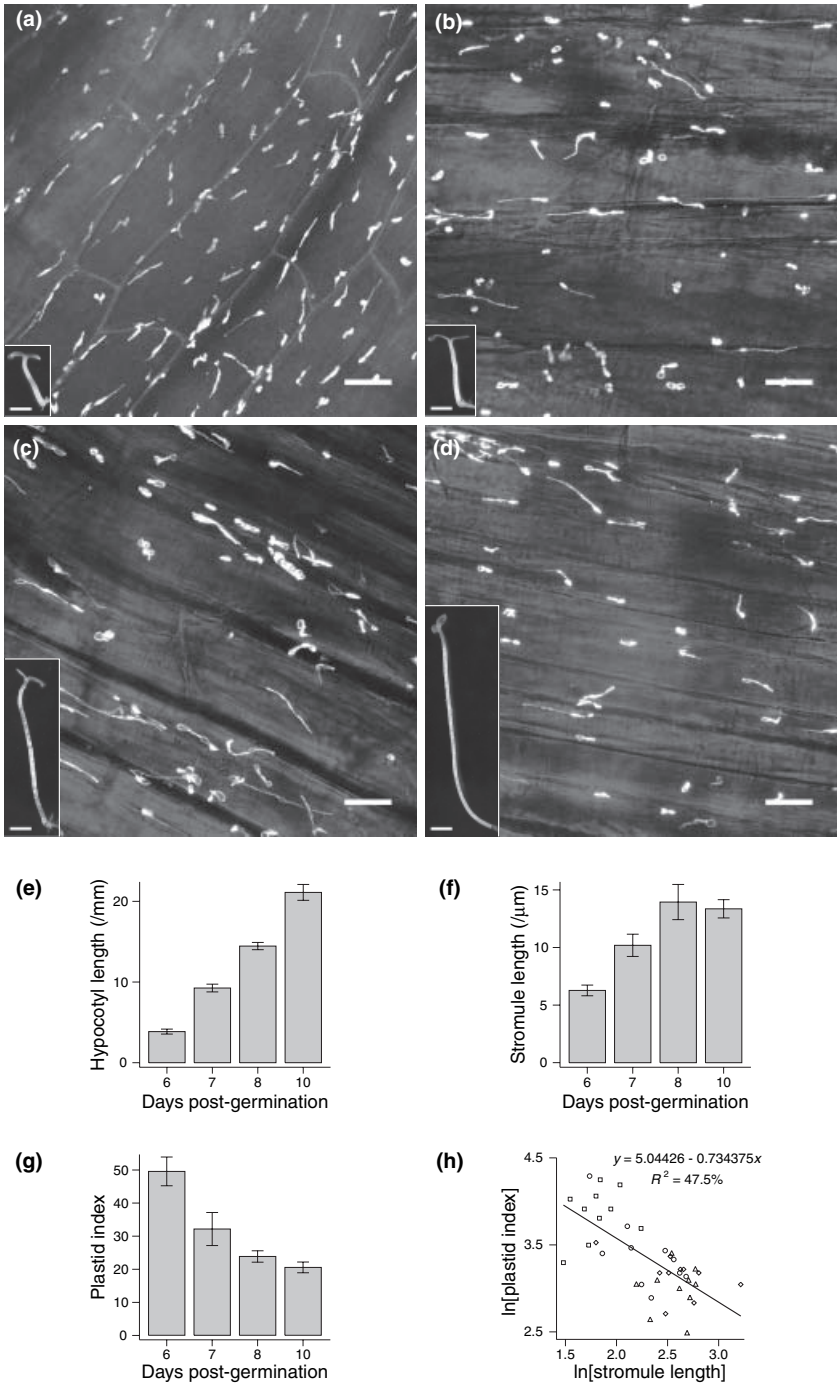

Figure 7. Stromule length is negatively correlated with plastid density.
Transplastomic tobacco seedlings expressing GFP were sown on nutrient agar and allowed to germinate in the dark for 5, 6, 7 or 9 days in order to induce hypocotyl elongation, followed by 1 day of light treatment to induce de-etiolation. (a–d) Stromules in hypocotyl epidermis (a) 6 days, (b) 7 days, (c) 8 days and (d) 10 days after sowing. Images are maximum projections of a confocal series along the *z*-axis, superimposed on a transmitted light image to highlight cell walls. Note that stromules are mostly orientated parallel to the lateral cell walls, running in parallel across each image. Note also that plastid count per unit area generally decreases and stromule length increases as the hypocotyl extends. Insets show representative seedlings for each treatment. Scale bars: 20 μm (insets 2 mm). (e) Hypocotyl length increases with duration of dark treatment. Bars indicate mean ± 1 SE, $n = 10$ seedlings. (f) Stromule length increases with duration of dark treatment. Bars indicate mean ± 1 SE, $n = 10$ images; up to 15 stromules were measured per image. (g) Plastid index, a measure of number of plastids per unit area, decreases with hypocotyl elongation. Bars indicate mean ± 1 SE, $n = 10$ images. (h) Stromule length is negatively correlated with plastid index. Note the logged scale. Squares, 6 days; circles, 7 days; diamonds, 8 days; triangles, 10 days. Each point represents the mean stromule length plotted against the stromule index for each image (10 images per treatment).

was a large degree of variability in stromule length with no significant difference between the two treatments (Mann–Whitney, $P > 0.05$; Figure 7f), despite a large difference in hypocotyl elongation. Plastid index decreased with hypocotyl length, although this also appeared to tail off between 8 and 10 dpg (Figure 7g). Finally, plotting stromule length against plastid index revealed a strong and significant negative correlation between the two factors ($P < 0.001$; Figure 7h). From these data we infer that long stromules are produced by plastids in response to a rapid decrease in plastid index, thus increasing the contact surface area between the plastid compartment and the rest of the cell.

Discussion

Previous studies into the distribution of stromules between different plastid and cell types have shown that they are highly variable for reasons which are unclear (Köhler and Hanson, 2000; Pyke and Howells, 2002). We describe here how plastid differentiation, plastid size and the density of plastids within the cell can independently influence the frequency and extent of stromules, thus providing insight into some of the developmental factors that regulate their formation.

Tomato fruit mesocarp contains two morphologically distinct populations of plastids, which differ in plastid size and number. Two types of tomato fruit chromoplast have been documented previously (Harris and Spurr, 1969; Rosso, 1967), which resemble closely the needle-like OM and ovoid IM chromoplasts described here. Moreover, Öztiğ (1962) noted that the chromoplast shape varies with position of the cell in the fruit. These two types of chromoplast are derived from progenitor chloroplasts that also exhibit dimorphism; however, we propose that the plastids present in IM cells of MG fruit are better considered as amyloplasts, for the following reasons. Firstly, both the presence of starch in these plastids of dark-grown fruit and the subsequent normal fruit ripening indicate that fruit photosynthesis is not essential for starch production or for fruit development. Secondly, tomato fruit are sink organs and no net photosynthesis occurs in MG fruits (Ho and Hewitt, 1986). IM plastids of MG fruit are thus atypical of chloroplasts in general, and therefore their morphology and associated stromules do not closely resemble those of other chloroplasts. Amyloplast stromules (Langeveld *et al.*, 2000) and protrusions containing starch grains (Bechtel and Wilson, 2003) have been reported in wheat endosperm, and estimates of the length of amyloplast stromules in this tissue range from 2 to 30 μm (Langeveld *et al.*, 2000), comparable with the IM cell plastid stromules from MG fruit.

The increase in stromule abundance during chromoplast differentiation only occurs in IM cells, suggesting that attainment of the chromoplast state *per se* is not sufficient for increased stromule abundance. This presents two aspects to be explained, namely why there exists such a dramatic difference in plastid morphology between OM and IM cells, and why the increase in stromule abundance is specific to IM cells. The plastid dimorphism originates from the early stages of fruit development, when starch distribution is non-uniform throughout the pericarp (Ho and Hewitt, 1986). It is unclear why the starch-storing plastids in IM cells should be less densely packed than non-storing ones of OM cells. Amyloplasts in wheat endosperm can be 10 μm or more in diameter (Langeveld *et al.*, 2000), probably as a result of the starch granule expansion. Rapid starch granule deposition in IM cell plastids may restrict plastid division while the cell continues to expand during fruit growth: a similar observation in wheat endosperm prompted Bechtel and Wilson (2003) to speculate that amyloplasts may divide by some form of budding. This decreased plastid number/increased plastid size then persists through to the chromoplast stage, resulting in the large ovoid chromoplasts typical of IM cells. In OM cells, however, where bulky starch granules do not restrict plastid division, the plastids are smaller and attain a higher number within the cell, and maintain this state as chromoplasts in ripe fruit.

The negative impact of chloroplast components on stromule formation further demonstrates that plastid differentiation is a major contributor to the process. Stromules are less common in IM cells of B + 7 *gf* fruit than in wild type because the plastids in these cells are still chloroplast-like in nature, and thus express some morphological features typical of chloroplasts. The *gf* mutation had no effect in OM cells, reflecting the relative constancy of plastid morphology in this tissue in wild type fruit. Similarly, the *rin* mutation shows how blocking plastid differentiation affects stromule formation. By B + 40 the plastid dimorphism in the mesocarp largely disappears, implying that substantial plastid division must have occurred post-breaker, especially in the IM cells. Stromules are also remarkably similar between the two cell types, with absolute differences being small. These observations suggest that the nature of plastid stromules is much more closely related to the differentiation status of the plastid in question rather than the cell type. By blocking chromoplast development, the morphology associated with chromoplasts and the two plastid populations are lost.

In general, smaller plastids produce the shortest stromules (Table 1), presumably because of the limited amounts of membrane available to be incorporated into them. However, while mesophyll chloroplasts are among the largest plastids in a plant, they produce relatively short stromules (Gray *et al.*, 2001), indicating that there must be other factors that control stromule formation. Little is known about the molecular regulation of plastid and organelle morphology in plants, but changes in membrane elasticity and amenability to distortion may be one

contributing factor to stromule formation. Members of the FtsZ family of proteins have been implicated in regulating chloroplast shape (Kiessling *et al.*, 2000). FtsZ proteins are involved in chloroplast division in both higher and lower plants, and share structural and functional similarity to tubulins (Osteryoung and McAndrew, 2001). Overexpression of an FtsZ-GFP fusion protein in *Physcomitrella patens* showed a filamentous, reticulate scaffold of FtsZ apparently just below the plastid envelope (Kiessling *et al.*, 2000), suggesting that plastids maintain their shape by means of a proteinaceous 'plastoskeleton', although this may be an artefact of FtsZ overexpression (Vitha *et al.*, 2001). Nevertheless, it has been confirmed that the actin cytoskeleton is at least partially responsible for stromule movement (Kwok and Hanson, 2003), so it is conceivable that the ability of actin microfilaments to distort the plastid membrane is related to its elasticity as determined by some plastidial structural component. Changes in stromule length and frequency may be a result of changes in plastid membrane amenability to deformation, increased plastid-cytoskeletal activity or a combination of both. In addition, the increase in chromoplast membrane availability may be enhanced by the break-up of thylakoid membranes and their incorporation into stromules. Accordingly, we suggest that OM cells of wild type fruit possess fewer and shorter stromules than IM cells because of a fundamental, developmentally early difference in plastid size and hence membrane availability. Upon ripening, the large IM plastids lose some chloroplast/amyloplast structural features and the plastid envelope attains a form more amenable to stromule biogenesis. Consequently, plastids at the transitional stages of chloroplast–chromoplast differentiation have intermediate forms.

The data from elongated tobacco hypocotyls indicate that the cellular density of plastids is another factor which determines stromule formation. Increased plastid surface area in these cells might be of particular importance as expanding cells require rapid synthesis and supply of fatty acids for incorporation into phospholipids (Neuhaus and Emes, 2000). While plastid density in dividing and expanding mesophyll cells remains approximately constant (Pyke, 1997) where maximal light interception is important, it is presumably more efficient for a hypocotyl epidermal cell to increase stromule abundance rather than maintain a high density of plastids. Similarly, it may be significant that stromules are aligned with the cell wall, thus supplying fatty acids close to their point of need; however, this may be an indirect effect of the orientation of the actin cytoskeleton and cytoplasmic streaming in general (Kwok and Hanson, 2004b). Notably, the tomato fruit data strongly support the tobacco data: long stromules are associated with plastids that are further apart, whereas short stromules are present in cells with a high density of plastids (Table 1). In IM cells, the increase in stromule membranes would improve metabolic contact between the plastid and the cytosol. In OM cells, higher density of plastids would not require this. In MG fruit, stromules may be important in starch generation, by acting as a surface for import of hexose phosphates from the cytosol. Once the fruit begins to ripen, stromules might provide greater import area for novel proteins involved in carotenoid biosynthesis and chromoplast differentiation (Camara *et al.*, 1995). In the case of an average IM cell chromoplast at B + 7, a single stromule of 30 μm in length occupies just 9% of the plastid volume, but constitutes some 34% of the total plastid surface area (assuming that the plastid body is a sphere and the stromule a uniform cylinder of 0.9 μm in diameter). Furthermore, stromules may assist in the co-ordination of plastid activities by reducing inter-plastid distances. Signalling between plastids may be important in regulating their cellular dynamics: rather like bacterial quorum sensing, plastids presumably need to assess their population level within the cell in order to initiate plastid division with appropriate timing.

Given that stromules are capable of transporting endogenous proteins such as Rubisco (Kwok and Hanson, 2004a) and that they increase the plastid surface area with minimal use of stromal volume, it is likely that they are adaptive features of the plant cell. Several aspects of stromule biology have been documented, including the molecular basis for their movement (Kwok and Hanson, 2003, 2004b) and their ability to transport macromolecules (Kwok and Hanson, 2004a), but little attempt has been made to explain their variability. Besides the factors discussed here, other determinants may play a role, such as the cell cycle. Recently, it has been demonstrated that plastids congregate in perinuclear regions in preparation for cytokinesis (Sheahan *et al.*, 2004); plastids in this position in leaf epidermal cells frequently exhibit stromules protruding towards the peripheral cytoplasm (Arimura *et al.*, 2001).

Currently, several questions regarding stromule biology remain unanswered. What, for example, determines whether a plastid produces many stromules as opposed to one long one? Is the direction of stromule outgrowth a random event that is dependent on cytoskeletal arrangement, or is there some form of specificity? How is the density of plastids sensed and integrated with the metabolic needs of the cell? Substantive progress in this field will require the identification of candidate proteins that directly regulate plastid form, and those that allow the plastid envelope to interact with the actin cytoskeleton.

Experimental procedures

Plant material

Tomato (*Lycopersicon esculentum* Mill. var. 'Ailsa Craig') seeds were sown in a 6:1 mixture of compost and perlite, and germinated under glasshouse conditions (minimum 16 h day regime,

24°C). Plants were allowed to grow to full maturity in 25 cm pots to maximize fruit yield, and fruit was sampled from the first or second truss. Transgenic tomato plants of wild type background, containing a construct targeting GFP to the plastid, were generated as described previously (Bird *et al.*, 1988; Pyke and Howells, 2002). The construct consists of the *Arabidopsis recA* transit sequence fused to the mGFP4 coding region, driven by a double CaMV 35S promoter (Köhler *et al.*, 1997). This construct was introduced into the *green flesh* and *ripening inhibitor* mutant backgrounds by crossing, using the mutants as the pollen recipient. The mutant lines are near-isogenic with the 'Ailsa Craig' background (Darby *et al.*, 1977). F_1 plants were screened for GFP fluorescence and selfed, and homozygous mutants were identified by means of their fruit phenotype in the F_2 generation. Analysis was carried out on F_3 individuals.

To obtain dark-grown fruit expressing the plastid-targeted GFP construct (wild type background), the first or second truss was covered with an A5-sized, brown paper envelope containing four sheets of A4 paper. This was then covered in one layer of aluminium foil and secured over the developing truss with masking tape, and tapped by hand every so often to promote pollination. Fruit were examined by microscopy at a stage equivalent to MG, as judged by the fruit on an untreated truss of a plant of similar age.

Tobacco seedlings contained a transgene integrated into the plastid genome, providing plastid-localized expression of GFP under the control of the ribosomal RNA operon promoter and *rbcL* leader sequence (Kahn and Maliga, 1999). Seeds were surface-sterilized by treatment in 10% bleach for 10 min, followed by three rinses with distilled water. The seeds were sown in 8 cm-high pots containing MSR3 media (4.2 g l^{-1} MS salts, 3% sucrose, 1 mg l^{-1} thiamine, 0.5 mg l^{-1} nicotinic acid, 0.5 mg l^{-1} pyroxidine, 7% agar) and stratified at 4°C for 2 days. The pots were exposed to light for 4 h to ensure germination, and then wrapped in two layers of foil for the relevant length of time. Pots were incubated at 24°C, and light was provided with a 16 h light/8 h dark regime.

Tissue sampling and microscopy

Fruit tissue from tomato plants was harvested and imaged immediately. Fruit pericarp was sliced in a longitudinal (i.e. apical-basal) direction using a sharp scalpel blade. Tissue was selected from regions of pericarp approximately equidistant from the stylar and penduncular poles of the fruit, and thin sections mounted on a glass slide in 10% glycerol. Using confocal microscopy, the upper 20–40 μm of individual pericarp cells were imaged as a Z-series and the component images (taken 1 μm apart) were merged to form a maximum intensity projection. Such images display the upper surface of the approximately spherical cell, with the plastids situated between the vacuole and the plasma membrane. Tobacco hypocotyls were imaged by dissecting the hypocotyl from the seedling before mounting. The upper 15–20 μm of the central region (i.e. midway between the root and cotyledonary tips) of the hypocotyl, encompassing the epidermis, was imaged. Confocal microscopy was performed with a Leica TCS2 confocal scanhead attached to a Leica DMRE upright microscope (Leica, Mannheim, Germany). GFP and chlorophyll were excited using the 488 nm line from the Ar laser, and emission signals were collected in separate channels, at wavelengths between 495 and 526 nm, and between 631 and 729 nm, respectively. Transmitted light was also collected in a separate channel. The GFP signal and chlorophyll autofluorescence were false-coloured green and red, respectively. Images shown are maximum intensity projections of optical slices produced by the LCS software provided. Epifluorescence microscopy was performed on a Nikon Optiphot microscope (Nikon, Kingston-upon-Thames, UK) with a DM 510 fluorescence filter block, and images were acquired using a Nikon DXM-1200 digital camera. Further image manipulation, including level adjustment and channel merging, was performed using Adobe Photoshop 7 (Adobe Systems Inc., San Jose, CA, USA).

Image analysis

Fruit were examined at four developmental stages: MG, 1 day post-breaker (B + 1), 3 days post-breaker (B + 3) and ripe (B + 7). The maximum intensity projections from the confocal microscope were imported into LUCIA G quantitative image analysis software (NIKON, UK) and quantified in various ways as follows. A 400 × 400 pixel square 'quadrat' (equivalent to 156 μm × 156 μm) was positioned over the centre of the imaged cell, and the proportion of plastids with stromules within the quadrat was recorded. A stromule was defined as any visible projection emanating from the surface of the plastid of less than 1 μm in diameter. Plastid index was defined as the number of plastids within the quadrat. In addition, stromule length was determined from up to 15 stromules from each image, and plastid plan surface area (estimated with a best fit 5-point ellipse) was determined as a mean of at least five plastids within the quadrat.

For tobacco seedlings the same methodology was employed, except that the quadrat was equivalent to 93 μm × 93 μm because of the higher magnification of the image. The quadrat covered several cells, and the term 'plastid index' equates to the number of plastids counted within the quadrat. Stromules were measured only on those plastids where the plastid body could be reasonably defined.

Statistical analysis

For each of the developmental stages considered, the mesocarp was divided into inner and outer regions based on the plastid dimorphism observed between them. At least 10 cells were measured from each developmental stage and region of the mesocarp considered (i.e. at least 20 cells per stage; see Table 1), sampling from at least four different fruit per stage. Each cell was considered an independent data point. For tobacco, 10 images per treatment were analysed, and each image was treated as an independent data point for stromule length and plastid index. Image analysis data were entered into MINITAB 13 statistical software (Minitab Inc., Philadelphia, PA, USA). The proportion of plastids with stromules was transformed with the angular transformation ($\sin\sqrt{X}$, where X is the proportion) to stabilize variance, creating a linear variable that we termed 'stromule index', which allows more valid comparison between treatments when displayed graphically. Stromule lengths were found to be right skewed and thus were transformed by converting to natural logarithms before statistical analysis was performed. To assess differences between plastid parameters, Mann–Whitney rank sum tests were utilized as this test requires the satisfaction of fewer assumptions.

Acknowledgements

The authors thank Maureen Hanson, Cornell University, Ithaca, for the gift of the plastid-targeted GFP construct. MTW is a grateful recipient of a Sainsbury PhD studentship funded by The Gatsby Charitable Foundation.

References

Akhtar, M.S., Golschmidt, E.E., John, I., Rodoni, S., Matile, P. and Grierson, D. (1999) Altered patterns of senescence and ripening in *gf*, a stay green mutant of tomato (*Lycopersicon esculentum* Mill.). *J. Exp. Bot.* **50**, 1115–1122.

Arimura, S.-I., Hirai, A. and Tsutsumi, N. (2001) Numerous and highly developed tubular projections from plastids observed in tobacco epidermal cells. *Plant Science*, **169**, 449–454.

Bechtel, D.B. and Wilson, J.D. (2003) Amyloplast formation and starch granule development in hard red winter wheat. *Cereal Chem.* **80**, 175–183.

Bird, C., Smith, C.J.S., Ray, J.A., Moureau, P., Bevan, M.W., Bird, A.S., Hughes, S., Morris, P.C., Grierson, D. and Schuch, W. (1988) The tomato polygalacturonase gene and ripening-specific expression in transgenic plants. *Plant Mol. Biol.* **11**, 651–662.

Bourett, T.M., Czymmek, K.J. and Howard, R.J. (1999) Ultrastructure of chloroplast protuberances in rice laves preserved by high pressure frezzing. *Planta*, **208**, 472–479.

Bramley, P.M. (1997) The regulation and genetic manipulation of carotenoid biosynthesis in tomato fruit. *Pure Appl. Chem.* **69**, 2159–2162.

Büker, M., Schünemann, D. and Borchert, S. (1998) Enzymic properties of developing tomato (*Lycopersicon esculentum* L.) fruit plastids. *J. Exp. Bot.* **49**, 681–691.

Camara, B., Hugueney, P., Bouvier, F., Kuntz, M. and Monéger, R. (1995) Biochemistry and molecular biology of chromoplast development. *Int. Rev. Cytol.* **163**, 175–247.

Cheung, A.Y., McNellis, T. and Piekos, B. (1993) Maintenance of chloroplast components during chromoplast differentiation in the tomato mutant *green flesh*. *Plant Physiol.* **101**, 1223–1229.

Cookson, P.J., Kiano, J., Fraser, P.D., Römer, S., Shipton, C.A., Schuch, W., Bramley, P.M. and Pyke, K.A. (2003) Increases in cell elongation, plastid compartment size and translational control of carotenoid gene expression underlie the phenotype of the *High Pigment-1* mutant of Tomato. *Planta*, **217**, 896–903.

Darby, L.A., Ritchie, D.B. and Taylor, I.B. (1977) Isogenic lines of tomato 'Ailsa Craig'. *Glasshouse Crops Res. Ann. Rep.*, 168–184.

Fraser, P.D., Truesdale, M.R., Bird, C.R., Schuch, W. and Bramley, P.M. (1994) Carotenoid biosynthesis during tomato fruit development. *Plant Physiol.* **105**, 405–413.

Gendreau, E., Traas, J., Desnos, T., Grandjean, O., Caboche, M. and Hofte, H. (1997) Cellular basis of hypocotyl growth in *Arabidopsis thaliana*. *Plant Physiol.* **114**, 295–305.

Gillaspy, G., Ben-David, H. and Gruissem, W. (1993) Fruits: a developmental perspective. *Plant Cell*, **5**, 1439–1451.

Gray, J.C., Sullivan, J.A., Hibberd, J.M. and Hansen, M.R. (2001) Stromules: mobile protrusions and interconnections between plastids. *Plant Biol.* **3**, 223–233.

Hanson, M.R. and Köhler, R.H. (2001) GFP imaging: methodology and application to investigate cellular compartmentation in plants. *J. Exp. Bot.* **52**, 529–539.

Harris, W.M. and Spurr, A.R. (1969) Chromoplasts of tomato fruits. II. The red tomato. *Am. J. Bot.* **56**, 380–389.

Hawes, C., Saint-Jore, C.M., Brandizzi, F., Zheng, H., Andreeva, A.V. and Boevink, P. (2001) Cytoplasmic illuminations: in planta targeting of fluorescent proteins to cellular organelles. *Protoplasma*, **215**, 77–88.

Hibberd, J., Linley, P., Kahn, M. and Gray, J. (1998) Transient expression of green fluorescent protein in various plastid types following microprojectile bombardment. *Plant J.* **16**, 627–632.

Ho, L.C. and Hewitt, J.D. (1986) Fruit development. In *The Tomato Crop* (**Atherton, J.G. and Rudich, J.**, eds). New York: Chapman and Hall, pp. 201–239.

Kahn, M.S. and Maliga, P. (1999) Fluorescent antibiotic resistance marker for tracking plastid transformation in higher plants. *Nat. Biotechnol.* **17**, 910–915.

Kiessling, J., Kruse, S., Rensing, S.A., Harter, K., Decker, E.L. and Reski, R. (2000) Visualization of a cytoskeleton-like FtsZ network in chloroplasts. *J. Cell Biol.* **151**, 945–950.

Köhler, R.H. (1998) GFP for in vivo imaging of subcellular structures in plant cells. *Trends Plant Sci.* **3**, 317–320.

Köhler, R.H. and Hanson, M.R. (2000) Plastid tubules of higher plants are tissue-specific and developmentally regulated. *J. Cell Sci.* **113**, 81–89.

Köhler, R.H., Cao, J., Zipfel, W.R., Webb, W.W. and Hanson, M.R. (1997) Exchange of protein molecules through connections between higher plant plastids. *Science*, **276**, 2039–2042.

Kwok, E.Y. and Hanson, M.R. (2003) Microfilaments and microtubules control the morphology and movement of non-green plastids and stromules in *Nicotiana tabacum*. *Plant J.* **35**, 16–26.

Kwok, E.Y. and Hanson, M.R. (2004a) GFP-labelled Rubisco and aspartate aminotransferase are present in plastid stromules and traffic between plastids. *J. Exp. Bot.* **55**, 595–604.

Kwok, E. and Hanson, M. (2004b) *In vivo* analysis of interactions between GFP-labeled microfilaments and plastid stromules. *BMC Plant Biol.* **4**, 2.

Langeveld, S.M.J., Van Wijk, R., Stuurman, N., Kijne, J.W. and de Pater, S. (2000) B-type granule containing protrusions and interconnections between amyloplasts in developing wheat endosperm revealed by transmission electron microscopy and GFP expression. *J. Exp. Bot.* **51**, 1357–1361.

Neuhaus, H. and Emes, M. (2000) Non-photosynthetic metabolism in plastids. *Annu. Rev. Plant Physiol. Plant Mol. Biol.* **51**, 111–140.

Osteryoung, K.W. and McAndrew, R.S. (2001) The plastid division machine. *Annu. Rev. Plant Physiol. Plant Mol. Biol.* **52**, 315–333.

Öztiğ, F. (1962) Sur la forme et l'origine des pigments dans la tomate mûr. *Adv. Front. Plant Sci.* **1**, 153–156.

Pyke, K. (1997) The genetic control of plastid division in higher plants. *Am. J. Bot.* **84**, 1017–1027.

Pyke, K.A. and Howells, C.A. (2002) Plastid and stromule morphogenesis in tomato. *Ann. Bot.* **90**, 559–566.

Römer, S., Fraser, P.D., Kiano, J.W., Shipton, C.A., Misawa, N., Schuch, W. and Bramley, P.M. (2000) Elevation of provitamin A content of transgenic tomato plants. *Nat. Biotechnol.* **18**, 666–669.

Rosso, S.W. (1967) An ultrastructural study of the mature chromoplasts of the tangerine tomato (*Lycopersicon esculentum* var. 'Golden Jubilee'). *J. Ultrast. Res.* **20**, 179–189.

Sheahan, M.B., Rose, R.J. and McCurdy, D.W. (2004) Organelle inheritance in plant cell division: the actin cytoskeleton is required for unbiased inheritance of chloroplasts, mitochondria and endoplasmic reticulum in dividing protoplasts. *Plant J.* **37**, 379–390.

Tigchelaar, E.C., McGlasson, W.B. and Buescher, R.W. (1978) Genetic regulation of tomato fruit ripening. *Hort. Sci.* **13**, 508–513.

Tirlapur, U., Dahse, I., Reiss, B., Meurer, J. and Oelmüller, R. (1999) Characterisation of the activity of a plastid-targeted green fluorescent protein in *Arabidopsis*. *European Journal of Cell Biology* **78**, 233–240.

Vitha, S., McAndrew, R. and Osteryoung, K. (2001) FtsZ ring formation at chloroplast division site in plants. *J. Cell Biol.* **153**, 111–119.

Vrebalov, J., Ruezinsky, D., Padmanabhan, V., White, R., Medrano, D., Drake, R., Schuch, W. and Giovannoni, J. (2002) A MADS-box gene necessary for ripening at the tomato *Ripening-inhibitor* (*Rin*) locus. *Science*, **296**, 343–346.

Waters, M.T. and Pyke, K.A. (2004) Plastid development and differentiation. In *Plastids* (**Møller, S.G.**, ed.). Oxford: Blackwell, pp. 30–59.